Supported Zeolite Membrane by Vapor-Phase Regrowth

C. S. Tsay and A. S. T. Chiang
Dept. of Chemical Engineering, National Central University, Chung-Li, Taiwan, R.O.C. 32054

A new method for preparing supported zeolite membrane is proposed. A layer of colloidal MFI zeolite is deposited on a porous ultrafiltration support, on which a silica barrier layer has been precoated. The composite is then heated at 100°C under saturate water vapor for 30 h to obtain a very thin zeolite membrane with a glassy look. Under SEM, the zeolite membrane exhibits obvious void when the particles deposited were 100 × 150 nm in size. The particles are packed much closer if 80 × 100-nm particles were used. With smaller (60 × 80 nm) particles, the boundary between particles fuses together, and a continuous zeolite membrane could therefore be prepared. The membrane thickness could also be reduced by depositing less colloidal zeolite for regrowth to obtain a continuous zeolite membrane as thin as 0.5 μm on top of a multilayer porous alumina support. Some preferred orientation of the elliptical zeolite particles is observed on the surface of the membrane, but no preferred crystallography orientation is confirmed. The reproducibility of this preparation method was checked by room temperature permeation measurements of several gases. Nearly identical results were obtained on two separately prepared membranes. Permeation results also confirmed that there were very few, if not free of, pinholes in the zeolite membrane so prepared.

Introduction

Zeolite films have attracted much attention in the last decade due to their potential as selective membranes, catalytic films, electrodes, sensors, and optoelectronic devices. Many methods have been proposed for the synthesis of zeolite film. They can be broadly classified into two groups according to whether or not the substrate is immersed in a precursor solution.

The *in situ* growth of zeolite film on an immersed substrate could be traced back to the early observation of zeolite coated on the Teflon lining of the reactor. By the early 1990s, several groups (Sano et al., 1991; Myatt et al., 1992; Kiyozumi et al., 1992; Geus et al., 1993; Jansen and Vanrosmalen, 1993) had succeeded in preparing a continuous zeolite coating on dense substrates. More recent studies (Scandella et al., 1996; Hedlund et al., 1997a; Boudreau and Tsapatsis, 1997; Koegler et al., 1997; Schoeman et al., 1997) had their emphasis on the control of the thickness and orientation of the coated zeolite film. In particular, many (Feng and Bein, 1997; Hedlun et al., 1997b; Sterte et al., 1997; Mintova et al., 1997a) have tried to separate the nucleation and growth processes by assembling zeolite nuclei on a dense substrate before immersing them in a precursor solution.

The decoupling of nucleation and growth by predeposition of seeds also worked for porous substrate. In the studies of Lovallo (Lovallo and Tsapatsis, 1996; Lovallo et al., 1998), a layer of colloidal zeolite was first deposited on a porous support. The composite membrane was then immersed in a precursor solution under hydrothermal conditions, so that the interparticle void could be eliminated by secondary growth. A rather thin membrane ($1 \sim 2$ μm) could be obtained with this approach, as compared to the >10-μm membrane produced in the earlier studies (Geus et al., 1992, 1993). A similar *in situ* secondary-growth method is also described in many recent patents (Lai, 1998; Lai et al., 1999; Ruderman et al., 1998).

However, the immersion of a porous support in a zeolite precursor solution may be complicated by two factors. First, the pores in the support may be plugged by the heterogeneous nucleation of zeolite under the regrowth condition. Since the plugging of support may be difficult to control, two similarly prepared samples may have very different permeation properties.

Correspondence concerning this article should be addressed to A. S. T. Chiang.

Second, some porous support may dissolve into the precursor solution and thus change the solution composition. This is particularly true when the support is γ-alumina and the desired zeolite is silicalite. The dissolution of γ-aluminum may lead to an undesirable aluminum distribution.

We therefore propose to treat the porous support/zeolite nuclei composite directly under saturated steam instead of immersing it in a precursor solution.

The proposed vapor-phase-regrowth method is, in some sense, similar to the vapor-phase-transport (VPT) method employed by others (Li et al., 1992, 1994; Matsukata et al., 1994a; Nishiyama et al., 1995, 1996; Mimura et al., 1996). In the VPT approach, however, the precursor is deposited on the substrate as a gel layer, which is then converted to zeolite under heated (water and template) vapor. Despite its name, neither the zeolite nuclei nor the nutrient is actually transported through the vapor phase. It has been argued (Sano et al., 1992a,b) that a condensed water layer is formed around the gel particles, which serves as a pool for the dissolution of gel and the crystallization (nucleation) of zeolite.

The VPT method has not been a popular way for the synthesis of zeolite membrane. One of the reasons for this may be that a rather thick gel film must be deposited on the substrate to produce a reasonable film of zeolite. This is associated with the large density difference between gel and zeolite. A thick but crack-free gel film is itself difficult to prepare. The large volume change when converted to zeolite further increases the chance it will crack.

By depositing zeolite nuclei instead of gel on a porous support, the difficulty of preparing a thick and crack-free gel film is avoided. Under saturated vapor, a condensed water layer can still be formed between zeolite particles, and the dissolution–recrystallization process will eliminate the interparticle void just as in the case of *in-situ* secondary growth.

The proposed vapor-phase-regrowth method had the additional benefit of precise thickness control. Since no precursor other than the nuclei themselves (aside from the silica underlayer discussed later) is supplied to the regrowth of the zeolite, the final thickness is precisely controlled. This is important for achieving reproducible results.

For the preparation of pure silica zeolite (MFI) membrane on γ-alumina support, the problem of aluminum migration had yet to be addressed. A sol-gel silica layer can be added between the γ-alumina support and the zeolite nuclei as a barrier. Such a barrier layer could be easily prepared following the method of Brinker et al. (1993). The silica layer so obtained has a typical pore size less than 2 nm, and can thus effectively retain the deposited nuclei as well as the condensed water layer. At the same time it can also serve as the nutrient for the regrowth of the deposited nuclei.

Experimental

Materials

Alumina Support. All alumina support used in this study was a homemade multilayer composite UF membrane. It was in disk shape with a dimension of 2 mm $\times$ 4 cm ϕ. The disk support was made of, successively, 50-μm presintered α-Al_2O_3 particles, 4 μm α-Al_2O_3 crystals, 1 μm α-Al_2O_3 crystals and a top layer of γ-Al_2O_3. The thickness of the last three layers were, respectively, 100 μm, 30 μm, and $\sim$0.5 μm. The biaxial flexure strength of this porous support was better than 20 MPa, comparable to most commercial products. Details of the procedures for preparing this UF support will be given elsewhere.

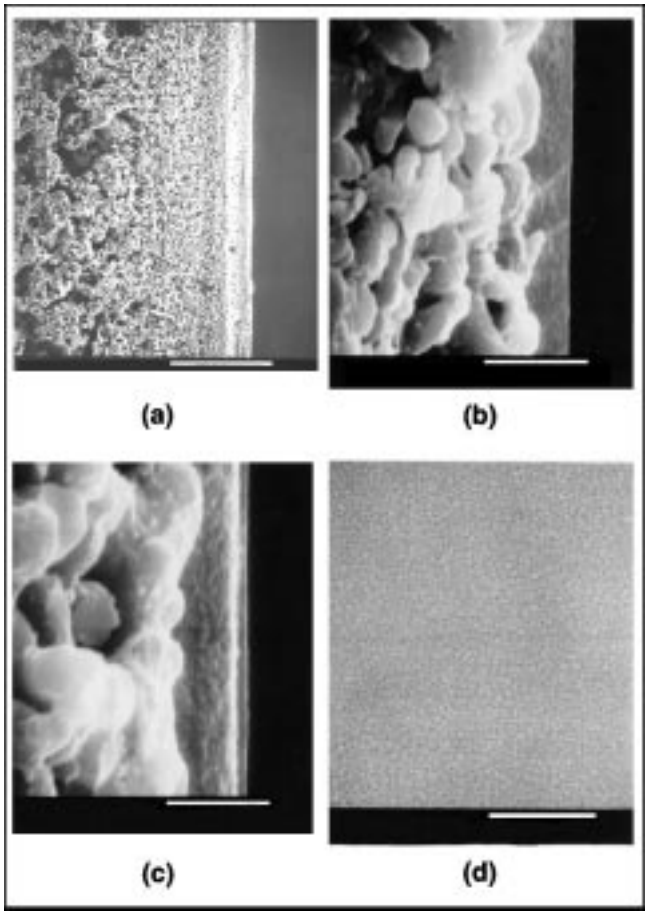

Figure 1. Cross section of (a) the support without the γ-Al_2O_3 layer; (b) the γ-Al_2O_3 top layer of the UF support; (c) the UF support after adding the silica barrier; (d) top view of the silica barrier layer.

The bars are 150 μm, 1.5 μm, 0.86 μm and 0.5 μm, respectively.

The cross-section view of a typical support disk is given in Figures 1a and 1b. Figure 1b clearly demonstrates a distinct γ-Al_2O_3 layer on top of the 1-μm α-Al_2O_3 crystal layer. Under higher magnification, this γ-Al_2O_3 film could be seen to consist of particles about 30 nm in size.

The reason for using such a complicated support needs some elaboration. If zeolite membrane is to be of any practical application, it must be thin enough to achieve a reasonably large flux. Ways to prepare ultrathin zeolite membrane are therefore of interest. To study the permeation of gases through a thin zeolite membrane, however, it is important that the permeance of the support is also large, so that the major flow resistance is at the zeolite layer rather than the support. A multilayer porous support is the only way we could achieve this requirement.

Silica Barrier Layer. Tetraethylorthosilicate (TEOS) and Methyl-triethoxy silane (MTES) were used to prepare the sil-

ica sol for coating the barrier layer. The procedure was similar to that of Brinker and his colleagues (Brinker et al., 1993; Raman and Brinker, 1995). Specifically, a solution with a molar composition of MTES/TEOS/EtOH/H_2O/HCl = 0.05/1/2.1/0.6/0.0039 was stirred and reacted at 50°C for 90 min. After cooling to room temperature, aqueous HCl was added so that the final composition became 0.05/1/2.1/2.22/0.256. The acidified sol had a viscosity $\sim$1.3 cp and pH $\sim$0.15. After about 3 h, it was further diluted with twice its volume of absolute ethanol. The diluted sol had a viscosity of $\sim$1 cp and pH $\sim$0.25. The SiO_2 content in the diluted sol was about 12 wt. %, and its viscosity never exceeded 2 cp, even after aging 24 h. This diluted sol was kept in a sealed bottle before use.

Colloidal Zeolite. The colloidal MFI zeolite used in this study was synthesized following our previous report (Tsay and Chiang, 1998). A clear solution was prepared by the hydrolysis of TEOS in a solution of tetrapropylammonium hydroxide (TPAOH). The molar composition was TEOS/TPAOH/H_2O = 1/X/20. The clear solution was subjected to hydrothermal reaction at 150°C in an autoclave. For $x = 0.2$ and a reaction time of 48 h, a colloid with $\sim$150 nm zeolite particles was obtained. For $x = 0.36$ and 25 h of reaction, the zeolite particles were about 80 nm in size, while the size increased to $\sim$100 nm if reacted for 30 h.

Membrane preparation

Silica Barrier Layer. The silica undercoat was applied by spin coating at 3000 rpm. The coated sample was aged at room temperature for 2 h and then calcined to 450°C (at 7°C/h and holding for 4 h). About 0.04 g (two drops) of the silica sol was enough to make a continuous layer $\sim 0.2\ \mu$m in thickness. Nitrogen adsorption measurement on a similarly dried and calcined gel piece from the same sol showed microporosity with pores of < 2 nm. This pore size was further confirmed by the permeation measurement of a silica-coated support.

Colloidal Zeolite Deposition. Only 0.36 mg of zeolite is needed to cover the disk support with a layer of the $\sim$150-nm zeolite particles. The zeolite colloid prepared as just described contains about 8 wt. % zeolite, which is too high to make such a deposition. Therefore, immediately before the depositing process, the as-prepared colloid is diluted with DI water 350 times its own weight. Notice that the original colloid was very stable at its pH value of 10 $\sim$ 11. After dilution, the pH value reduced to about 9.5, and the suspension became less stable. The colloidal particles will slowly settle down in more than a few hours. This is exactly what one needs to make a good deposition.

The support with the silica undercoat was first dried at 80°C. A piece of Scotch tape was wrapped around its circumference to make a cup for the colloidal zeolite. The calculated amount of diluted zeolite colloid was poured into this cup. The whole assembly was then left to stand for more than a day. Due to its small pore size, the silica barrier layer was almost impermeable to water. It took more than 5 h for a 0.5-cm-deep colloid to dry. At the same time, the zeolite particles settled into a rather dense film on the substrate.

Vapor Phase Regrowth of Zeolite Film. The support with a deposited zeolite film was placed on a Teflon hourglass, then in a 500-mL stainless steel (S.S.) autoclave. To the bottom of this autoclave, 0.5 g of DI water was added. The autoclave was sealed and heated to 100°C for 30 h. After cooling to room temperature in the oven, the composite membrane was retrieved and calcined at 7°C/h to 120°C, then at 8°C/h to 500°C, holding for 5 h, cooled down to 300°C at 10°C/h, and finally oven-cooled to room temperature. The entire zeolite membrane thus obtained showed a glassly layer on top.

Membrane Analysis. All zeolite membranes prepared were examined by a *Siemens D-500* XRD with Cu-Kα radiation. The measurement was made under 2θ mode, with a fixed incident angle of 0.05 degree. SEM analysis was made with a *Hitachi S-800* field emission electron microscope. The room-temperature permeance of several simple gases was measured. To obtain the true permeability of the zeolite membrane, the flow resistance of the support was also measured and subtracted from the overall resistance.

Results and Discussion

Silica barrier layer

The cross section and the surface morphology of the membrane after the silica coating are showed in Figures 1c and 1d. The silica barrier layer showed in this picture is about 100 nm thick. The surface appears to be tightly packed with particles about 20 nm in size, but the adsorption and permeation studies show only 2-nm pores. Therefore, the barrier layer must be denser inside.

Zeolite membrane after vapor-phase regrowth

A sample made with $\sim$150-nm zeolite particles and the vapor-phase regrowth process is shown in Figure 2. The first thing to be noticed is the elliptical shape of the zeolite particles making up these membranes. Therefore, the actual size of these particles should be 100×150 nm. The sample shown in Figure 2a was made with only 0.5 g of the diluted colloid, so that the amount of zeolite was not enough to cover the support surface. We find that most particles had their longer axis lying flat on the substrate. The silica barrier layer beneath, and its fusion with zeolite particles, is also clearly demonstrated.

When the amount of zeolite colloid deposited increases to 3.5 g, the surface of the membrane is completely covered, as shown in Figure 2b. This sample has been tilted a small amount to reveal the coverage away from the edge. Notice that the silica barrier no longer appears as a distinct layer in this picture. It may have been consumed by the growth of zeolite particles, since more particles have been deposited. The size of the zeolite particles observed in these pictures (150×190 nm) is indeed larger than that in the previous picture.

At a higher magnification (Figure 2c), one finds that the surfaces of the zeolite particles is covered with tiny bumps about 10 nm in size. Without other evidence, one would guess that they are the silica particles that originally existed in the barrier layer. However, we have found the same morphology on zeolite particles deposited directly on glass. We are thus sure that the rough surface is a property of the zeolite particles themselves. A similar scale of roughness has also been observed by Mintova et al. (1997b) in their zeolite film pre-

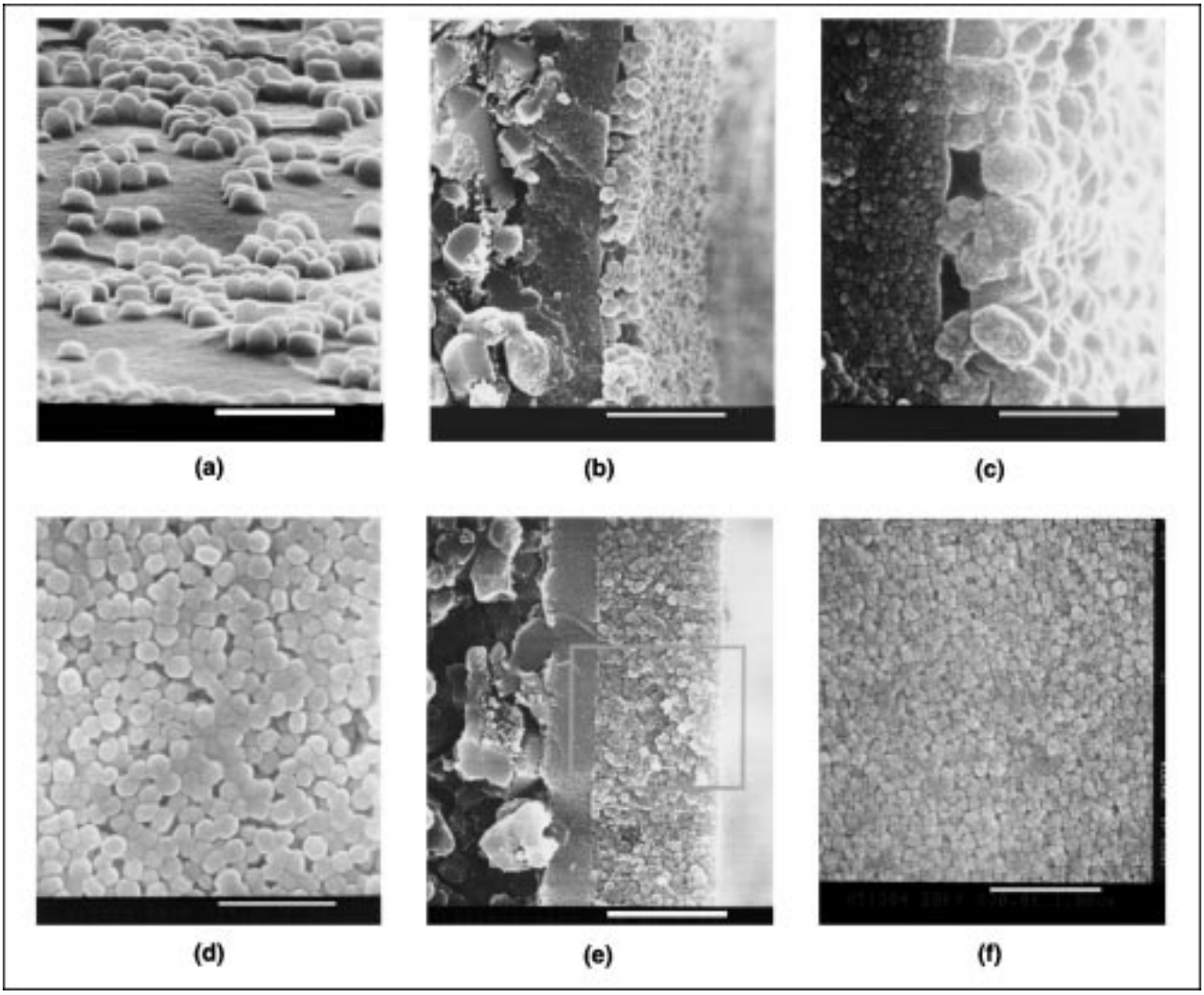

Figure 2. Membranes produced with (a) 0.5 g, (b, c, d) 3.5 g, (e, f) 25 g of the 100×150-nm colloidal zeolite.

The bars are 0.86 μm, 1.5 μm, 0.5 μm, 1.2 μm, 2.0 μm and 1.0 μm, respectively.

pared on a gold substrate. Most likely, the zeolite particles are agglomerates of smaller crystallites.

As shown in Figure 2d, the interparticle void of the membrane produced by the 100×150 nm seed particles is not completely sealed. Open pores clearly exist. One of the ways to reduce the pinhole is to make the membrane thicker. As the amount of colloid used increased to 25 g, a rather thick layer of zeolite membrane was obtained (Figure 2e). The surface of this membrane (Figure 2f) is indeed less porous than the previous case, and looks very similar to the result of Mintova et al. (1997b). In their study, the self-assemble-monolayer (SAM) technique was used to deposit the zeolite seeds before an *in situ* regrowth. Particles of different sizes were observed in their film, however, possibly due to the formation of new zeolite by heterogeneous nucleation.

Notice that the surface particles in Figure 2f are smaller than those in Figure 2d. Since these two samples have been made from the same colloid, the difference calls for an explanation. As we have mentioned, the zeolite particles can grow at the expense of the silica barrier layer. The surface particle of a thicker membrane can grow more slowly due to the longer path for the nutrient supply. There is another possibility, which is related to the elliptical shape of the zeolite particles: the particles at the surface may look smaller from the top simply because they have been oriented with the smaller projection facing up.

Whatever the case, the zeolite membranes prepared by the deposition of 100×150-nm colloidal particles were not satisfactory. We concluded that the particles were too large to make a pinhole-free membrane, and smaller particles should be used instead.

The results obtained with the smaller 60×80-nm and 80×100-nm particles are shown in Figure 3. The sample demonstrated in Figure 3a has been prepared with just 2 g of diluted 60×80-nm colloid. The zeolite membrane is barely two particles thick. There was a lighter colored region beneath the zeolite particles, which may correspond to the silica barrier layer. Interestingly, the particles at the membrane sur-

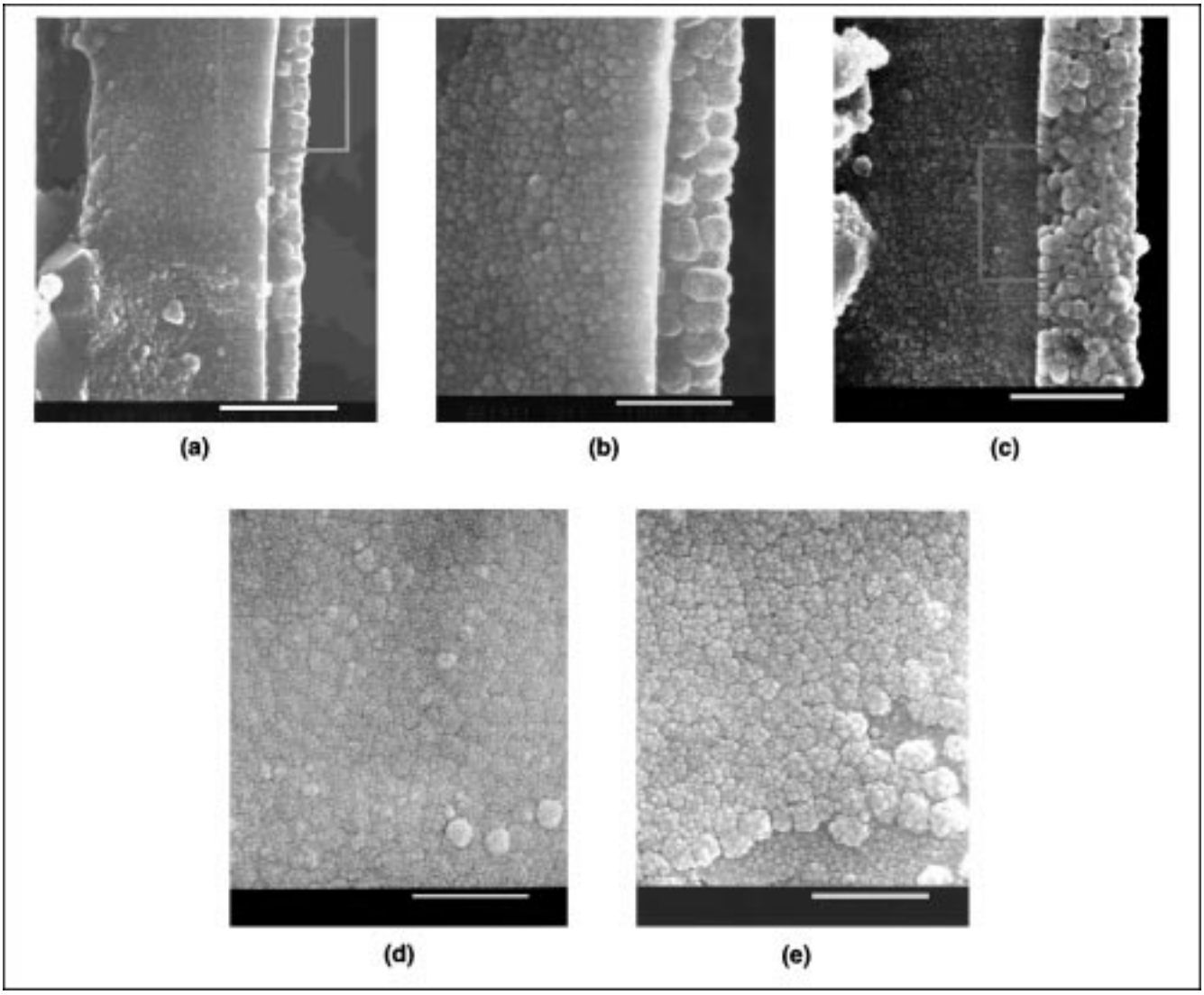

Figure 3. Membranes produced with (a, b) 2 g, (c, d) 5 g of the 60×80-nm colloidal zeolite, and (e) 5 g of the 80×100-nm colloidal zeolite.

The bars are 0.6 μm, 0.3 μm, 0.75 μm, 0.43 μm and 0.43 μm, respectively.

face seem to align in the same direction. The alignment of zeolite particles is more clearly shown in the enlarged picture (Figure 3b), where the $\sim$30-nm γ-Al_2O_3 particles and the finer features of the silica undercoat are somewhat visible. Again, zeolite particles immediately in contact with the silica layer are mostly lying flat, while most particles at the surface stand up.

The orientation of particles suggests that there may be an attractive force between the silica barrier and the zeolite particles. If this attractive force of the silica barrier is stronger than that of the other particles, the particle will lie flat on the silica. The gas/solid interface, on the other hand, does not attract zeolite particles. Thus, only the interparticle attraction acts on the surface layer. The particles are therefore aligned with the longer axes parallel to each other.

By depositing more zeolite particles, a 0.5-μm-thick zeolite membrane has been made, as shown in Figure 3c. This picture shows that the packing density of the 60×80-nm particles is much higher than that of the 100×150-nm particles.

If the interparticle attraction was the reason for the particle alignment on the membrane surface, it should be the same for a thicker membrane. This is indeed the case, as demonstrated in Figure 3d. In this picture, one finds that the zeolite particles on the surface are packed so tightly that the $<$10-nm primary crystallites practically cover the entire surface. The boundary between the 60×80-nm particles has almost disappeared. There is also a certain hexagonal pattern hinted in this picture.

The surface of a membrane made form 80×100-nm colloidal zeolite is given in Figure 3e. Comparing Figures 3d, 3e, 2d, and 2f, it is clear that the surface of the zeolite membrane becomes more tightly packed as the size of the zeolite particles become smaller. A pinhole-free membrane can only be produced when the particles are smaller than 100 nm. This

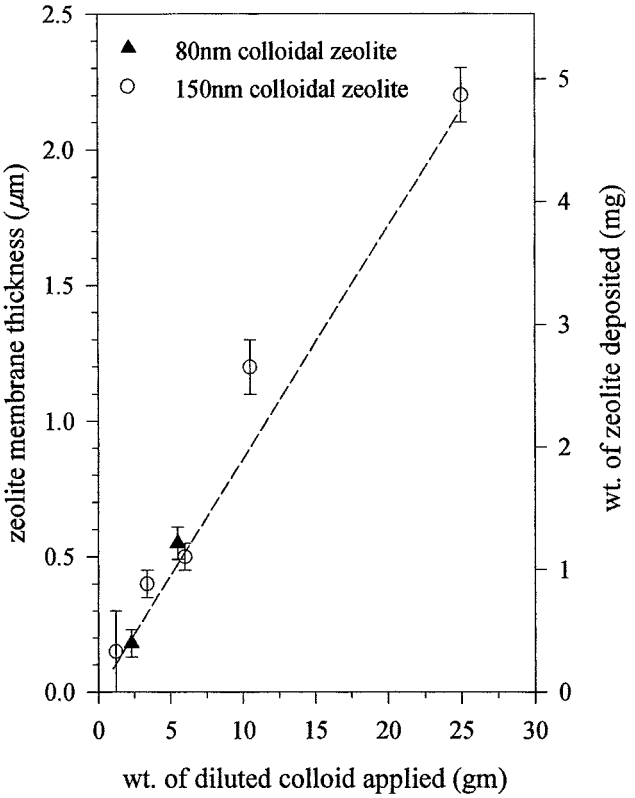

Figure 4. Variation of zeolite membrane thickness with the amount of diluted colloidal zeolite poured over the support.

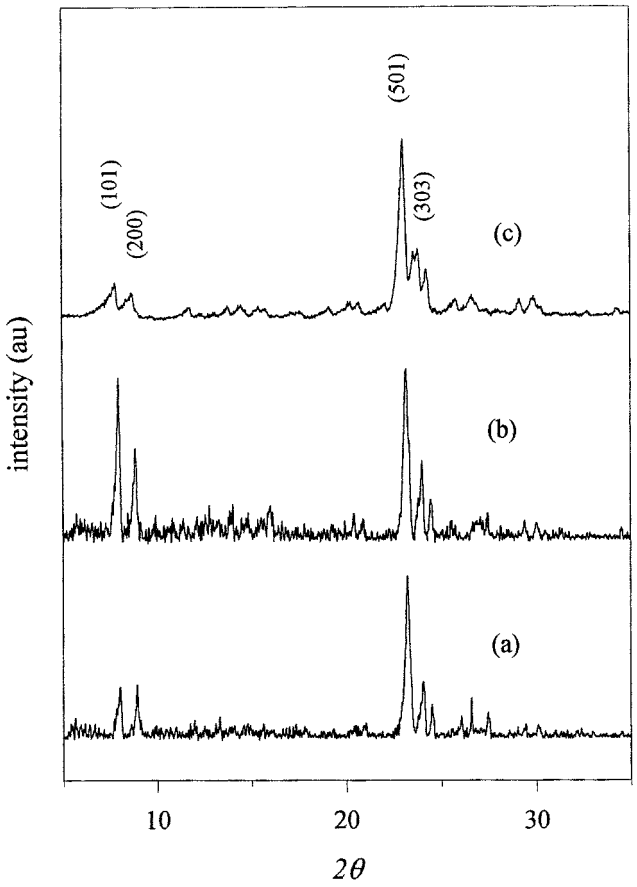

Figure 5. XRD patterns measured on (a) 2-μm-thick, (b) 0.5-μm-thick membrane produced from 60$\times$ 80 nm colloidal zeolite, and (c) powder of the same zeolite particles.

is in accordance with the conclusion made by Jansen and Vanrosmalen (1993).

The relations between the zeolite membrane thickness (from SEM) and the weight of the diluted colloid used are given in Figure 4. Clearly, the observed thickness of the zeolite membrane is directly proportional to the amount of zeolite deposited. Based on the density of zeolite MFI and the volume of the zeolite membrane, a porosity of < 0.1 is obtained for the membranes made by 60$\times$80-nm particles.

Crystal orientation in the membrane

The alignment of zeolite particles does not necessarily imply that the zeolites are crystallographically aligned. Nevertheless, the elliptical shape of the particle does suggest a possibility of a preferred crystalline axis. If this is the case, the membrane may also show a preferred crystalline direction under X-ray analysis.

Such a preferred direction would be difficult to detect, since the primary crystallites are no bigger than 10 nm, and those particles away from the surface may not be perfectly aligned. Clues about the possibly preferred crystalline direction may still be extracted, however, if we compare the XRD peaks of a thicker membrane with that of a thinner one, since a higher percentage of particles is aligned in the later case.

The XRD patterns of two zeolite membranes with different thicknesses are given in Figure 5, as is that of the original 60$\times$80-nm colloidal zeolite in powder form. Both the (101) and (200) peaks show a somewhat higher relative intensity for the 0.5-μm-thick membrane (Figure 5b) as compared to the zeolite powder (Figure 5c). Enhancement of (101)—together with (303)—would indicate a preferred crystal orientation with the *c*-axis tilted about 34° out of the normal-to-surface direction (Gouzinis and Tsapatsis, 1998). On the other hand, enhancement of (200)—together with (400)—would indicate a preferred crystal orientation with the normal-to-surface *a*-axis or *b*-axis (Tricoli et al., 1997). Since none of these patterns is clearly established in our XRD results, no reliable conclusion can be drawn.

Gas permeation studies

The overall room-temperature permeance of several gases through the support and the composite zeolite membrane are compared in Figure 6. The zeolite membrane used in these studies is a 0.5-μm-thick one, as shown in Figures 3c and 3d. The error bars given in Figure 6 have been estimated from the detection limits of the flow rate and the pressure. Notice that the permeability of our homemade UF membrane is relatively high compared to most commercial alumina UF membranes. Therefore, the major flow resistance of the composite is the zeolite membrane, even it is very thin.

For both the UF membrane and the composite zeolite membrane, two samples have been prepared and measured.

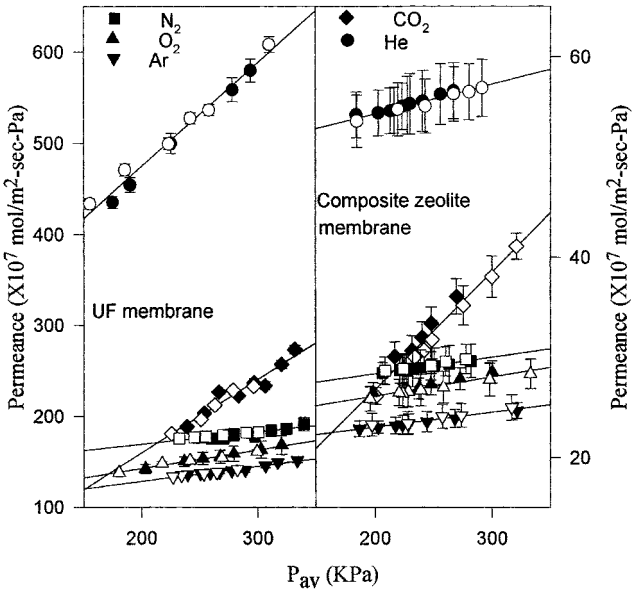

Figure 6. Room-temperature permeance of gases through (a) the UF support and (b) the composite zeolite membrane.

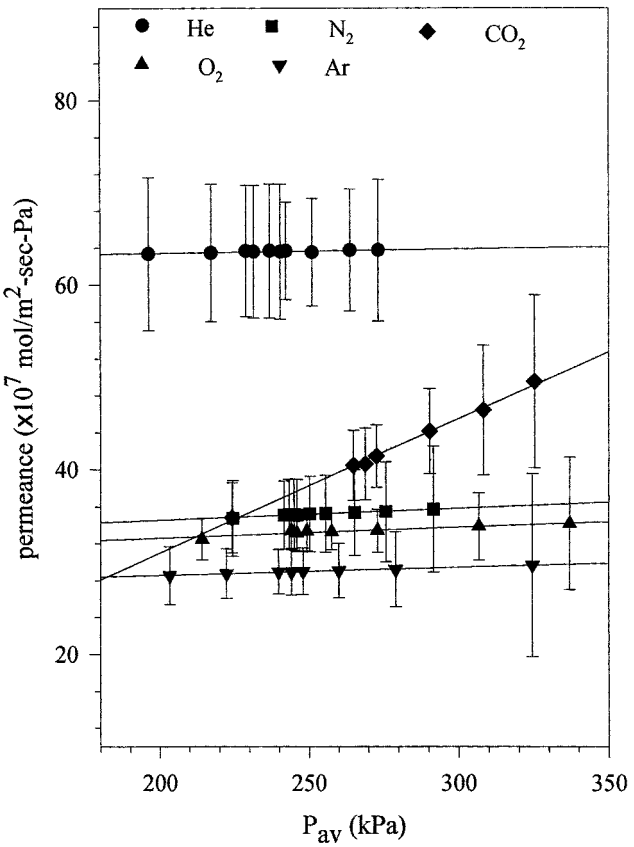

Figure 7. Calculated room-temperature permeance of gases through the zeolite membrane.

As shown by the different symbols in Figure 6, the permeation results of two samples coincide within the experimental error. This confirms the very important fact that the vapor-phase-regrowth method is reproducible.

The gas permeance through the alumina support shows strong pressure dependence, indicating that the main contribution is Poiseuille flow. However, the very strong pressure dependency of CO_2 permeance requires a different explanation. Because of its higher boiling point, CO_2 would be easily adsorbed or condensed in the micropores. The adsorption isotherm in the pressure range studied is most likely nonlinear. The permeance of CO_2 is therefore affected by both the surface flow and the nonlinearity of the adsorption isotherm, as discussed by others (Burggraaf et al., 1998).

For the zeolite membrane itself, there should be no Poiseuille flow. However, as a composite membrane, the overall permeance does vary with pressure due to the presence of the support. The pressure dependence would be small if the major flow resistance is that of the zeolite membrane. The true permeance of the zeolite membrane can be obtained by subtracting the contribution of the support from the overall resistance. The results of this calculation are shown in Figure 7. Notice that when subtracting two numbers, the associated error should be added. Therefore, the error bar in Figure 7 is larger than that in Figure 6.

For all gases studied but CO_2, the true permeance of the zeolite membrane is indeed pressure independent within the limit of experimental error. This is a good indication that our zeolite membranes are pinhole-free. Of course, more conclusive evidence could have been obtained if we had used a larger molecule for the permeance study, such as was done by Burggraaf et al. (1998).

For CO_2, a strong pressure dependency is still observed after the subtraction of support effect. A major part of this pressure dependency can again be attributed to the stronger and nonlinear adsorption of CO_2, but this may not be the whole story. Since the exothermic adsorption and the endothermic desorption occurred at the two faces of the membrane simultaneously, the heat transfer rate across the membrane may also play a role.

The permeability (with unit of $mol \cdot m/Pa \cdot s \cdot m^2$) of the zeolite membrane can be obtained by multiplying the permeance with its thickness. This permeability should be independent of the membrane thickness if the material is the same. Table 1 compared the gas permeability of our MFI zeolite membrane with that in the literatures. In some studies, the permeance was given without the membrane thickness. Those studies are thus not included, despite their good result. Furthermore, much of the literature has reported only an overall permeance of the composite membrane without substracting the effect of the support. Since the support only adds to the resistance, the permeability result in these studies should be considered as the lower limit for their zeolite membranes. Finally, the thickness taken here is usually the geometric one observed with a microscope, but the effective membrane thickness may be much smaller.

The permeability listed in this table spans several orders of magnitude. The large difference among the results in the literature reflects the fact that no two membranes are the same. Not only do the results vary with different authors, but also with the samples prepared by the same authors using the same techniques. In this respect, the reproducible permeation results obtained on our samples suggest a major improvement.

Table 1. Comparison of Gas Permeability Through MFI (*ZSM-5) Membrane

Authors	Support	MFI Memb. Thickness (μm)	Pressure and Temp.	Permeability $\times 10^{13}$ (mol·m/Pa·s·m^2) H_2	He	N_2	O_2
Uzio et al. (1994)	α-Al_2O_3 tube (SCT)	*300	303 K	—	—	15,600	
Coronas et al. (1997)	γ-Al_2O_3/α-Al_2O_3 tube (U.S. Filters)	* ~ 30 Si/Al = 100	300 K	540	—	177	—
		* ~ 30 Si/Al = 600	300 K	1080	—	330	—
Petersen and Peinemann (1996)	Alumina/Silica	*25	RT. 45 kPa		241	68.8	66.8
			RT. 10 kPa		156	54	52
Bai et al. (1995)	γ-Al_2O_3/α-Al_2O_3 tube (U.S. Filters)	~ 10	298 K ΔP = 60−100 kPa	340			
Piera et al. (1998)	α-Al_2O_3 tube (SCT)	~ 30 (SIL-A-1)	298 K, 101 kPa			93	27
		~ 30 (SIL-A-2)	298 K, 101 kPa			72	
	γ-Al_2O_3/α-Al_2O_3 tube (SCT)	~ 15	296 K, 101 kPa			120	
Jia et al. (1994)	γ-Al_2O_3/α-Al_2O_3 tube (U.S. Filters)	~ 5	298 K 120/0.082 kPa	220	134	78	
Geus et al. (1992)	Clay	* ~ 100	294 K 200/0.002 kPa	82		27	
Kusakabe et al. (1996)	α-Al_2O_2 tube	~ 60	303 K		33	18	
		~ 40	303 K			22.8	
Nomura et al. (1997)	ø5 cm SS disk 10-μm pore	~ 30, (16 h CVD)	298 K		15	22	
Matsukata et al. (1994b)	α-Al_2O_3 disk (Nihon Gaishi Co.)	**20	298 K, —			17	12
Oh et al. (1997)	α-Al_2O_3 tube (Dongsu Ind.)	*7	300 K, 100 kPa	47	28	16	18
Our membrane	γ-Al_2O_3/α-Al_2O_3 ø 40×2 mm UF disk	0.5	298 K, 270 kPa		32	17	16
Kusakabe et al. (1997)	α-Al_2O_3 tube	~ 20	303 K			12.3	
Zhang et al. (1996)	α-Al_2O_3 tube	~ 10	433 K			9.7	
Jia et al. (1993)	α-Al_2O_3 disk (KPM)	~ 5	293 K, 150 kPa	12	8.7	3.8	
Yan et al. (1995a,b)	α-Al_2O_3 disk (Coors Ceramic Co.)	* ~ 10 (# M3)	303 K ΔP = 127 kPa	6.2	3.0	3.2	3.7
Kiyozumi et al. (1997)	No support	60	298 K, 101 kPa			0.85	0.78
		65	298 K, 101 kPa			0.81	0.58
Lovallo and Tsapatsis (1996)	Silicalite + γ-alumina	0.75	458 K, 101 kPa	0.93		0.013	0.026
		1.5		0.29		0.0056	0.014
		2		0.38		0.007	0.022
Lovallo et al. (1998)	ø3 cm α-Al_2O_3 disk (Coors Ceramic Co.)	2.1 (#2)	290 K	1.8		0.63	0.67
		1.4 (#1)	400 K	0.294		0.007	0.015

Among the collected data, those reported by Gues (1992) and Kiyozumi et al. (1997) should be free of the influence of support. The former was made on a very thick piece of intergrown zeolite, while the latter used no support at all. These results were then taken as reasonable upper and lower limits, respectively, for the permeability of the MFI membrane. With this understanding, it was tempting to think that studies with permeability higher than that of Gues might have pinholes.

On the other hand, the results of Lovallo and coworkers (Lovallo and Tsapatsis, 1996; Lovallo et al., 1998) were a thousand times smaller than that of Kiyozumi. Since the data given in their studies were the overall permeance of a composite membrane, their support must have contributed much to the observed flow resistance. Notice further that their measurements were made at a higher temperature range than the others. According to their results, however, the gas permeation is an activated process, and the permeability can only be lower if brought to room temperature.

The two membranes prepared by Lovallo et al. (1998) were made by the *in situ* secondary growth of the seed layer. As their data suggested, the two samples prepared by the same procedure gave rather different results. A likely reason for the difference may be the plugging of support by the heterogeneous nucleation of zeolite during the *in situ* regrowth. By performing the regrowth process in the vapor phase, we may have eliminated this problem, and thus made the process more reproducible.

Conclusion

For the preparation of alumina-supported MFI zeolite membrane, the regrowth of seed crystals in the vapor phase

has at least two benefits compared to that in the liquid phase. First, the problem of support plugging, if it is an important one, can be eliminated. Second, direct control of the membrane thickness can be achieved by gauging the amount of seed deposited. With these improvements, zeolite membranes with reproducible gas permeance have been made.

We believe that the addition of a silica barrier layer on the porous support was a crucial step. A condensed liquid film should form on top of this silica layer during the vapor regrowth process. Due to the very fine pore structure of this silica layer, not only were the zeolite seeds retained above, but also the dissolved species was kept in the liquid film. Therefore, the seeds were constantly immersed in a saturated liquid film, so that the interparticle voids could be eliminated by regrowth.

For the vapor-phase-regrowth process, the colloidal zeolite must be smaller than 100 nm to produce a continuous membrane. We have demonstrated that membrane made from 80-nm particles is almost pinhole-free. The lower limit of the colloidal zeolite may be the ''nanoslab,'' with dimensions of $1.3\times4\times4$ nm, recently proposed by Ravishankar et al. (1999). If such a small unit were to be deposited, application of the silica barrier would be even more important.

Acknowledgments

This research was supported by the National Science Council of ROC through Grants NSC84-2214-E008-016, NSC85-2214-E008-010, and NSC86-2214-E008-002.

Literature Cited

Bai, C. S., M. D. Jia, J. L. Falconer, and R. D. Noble, ''Preparation and Separation Properties of Silicalite Composite Membranes,'' *J. Membr. Sci*., **105**, 79 (1995).

Boudreau, L. C., and M. A. Tsapatsis, ''Highly Oriented Thin-Film of Zeolite-A,'' *Chem. Mater*., **9**, 1705 (1997).

Brinker, C. J., T. L. Ward, R. Sehgal, N. K. Raman, S. L. Hietala, D. M. Smith, D. W. Hua, and T. J. Headley, ''Ultramicroporous Silica-Based Supported Inorganic Membranes,'' *J. Membr. Sci*., **77**, 165 (1993).

Burggraaf, A. J., Z. A. E. P. Vroon, K. Keizer, and H. Verweij, ''Permeation of Single Gases in Thin Zeolite MFI Membranes,'' *J. Membr. Sci*., **144**, 77 (1998).

Coronas, J., J. L. Falconer, and R. D. Noble, ''Characterization and Permeation Properties of ZSM-5 Tubular Membranes,'' *AIChE J*., **43**, 1797 (1997).

Feng, S., and. T. Bein, ''Growth of Oriented Molecular-Sieves on Organic Layers,'' *Stud. Surf. Sci. Catal*., **105**, 2147 (1997).

Geus, E. R., M. J. Denexter, and H. Vanbekkum, ''Synthesis and Characterization of Zeolite (MFI) Membranes on Porous Ceramic Supports,'' *J. Chem. Soc. Faraday Trans*., **88**, 3101 (1992).

Geus, E. R., H. Vanbekkum, W. J. W. Bakker, and J. A. Moulijn, ''High-Temperature Stainless Steel Supported Zeolite (MFI) Membrane: Preparation, Module Construction, and Permeation Experiments,'' *Microporous Mater*, **1**, 131 (1993).

Gouzinis, A., and M. Tsapatsis, ''On the Preferred Orientation and Microstructural Manipulation of Molecular Sieve Films Prepared by Secondary Growth,'' *Chem. Mater*., **10**, 2497 (1998).

Hedlund, J., B. J. Schoeman, and J. Sterte, ''Ultrathin Oriented Zeolite Lta Films,'' *Chem. Commun*., 1193 (1997a).

Hedlund, J., B. J. Schoeman, and J. Sterte, ''Synthesis of Ultra-Thin Films of Molecular-Sieves by the Seed Film Method,'' *Stud. Surf. Sci. Catal*., **105**, 2203 (1997b).

Jansen, J. C., and G. M. Vanrosmalen, ''Oriented Growth of Silica Molecular-Sieve Crystals as Supported Films,'' *J. Cryst. Growth*, **128**, 1150 (1993).

Jia, M. D., B. S. Chen, R. D. Noble, and J. L. Falconer, ''Ceramic-Zeolite Composite Membranes and Their Application for Separation of Vapor Gas-Mixtures,'' *J. Membr. Sci*., **90**, 1 (1994).

Jia, M. D., K. V. Peinemann, and R. D. Behling, ''Ceramic Zeolite Composite Membranes—Preparation, Characterization and Gas Permeation,'' *J. Membr. Sci*., **82**, 15 (1993).

Kiyozumi, Y., F. Mizukami, K. Maeda, T. Kodzasa, M. Toba, and S. Niwa, ''Synthesis of Oriented Zeolite Film on Mercury Surface,'' *Stud. Surf. Sci. Catal*., **105**, 2225 (1997).

Kiyozumi, Y., I. Mukoyoshi, T. Sano, and F. Mizukami, ''Synthesis of SAPO-N Polycrystalline Films,'' *Nippon Kagaku Kaishi*, 877 (1992).

Koegler, J. H., A. Arafat, V. Vanbekkum, and J. C. Jansen, ''Synthesis of Films of Oriented Silicalite-1 Crystals Using Microwave-Heating,'' *Stud. Surf. Sci. Catal*., **105**, 2163 (1997).

Kusakabe, K., S. Yoneshige, A. Murata, and S. Morooka, ''Morphology and Gas Permance of ZSM-5-Type Zeolite Membrane Formed on a Porous α-Alumina Support Tube,'' *J. Membr. Sci*., **116**, 39 (1996).

Kusakabe, K., A. Murata, T. Kuroda, and S. Morooka, ''Preparation of MFI-Type Zeolite Membranes and Their Use in Separating N-Butane and I-Butane,'' *J. Chem. Eng. Jpn*., **30**, 72 (1997).

Lai, W. F., ''Low Alkaline Inverted In-Situ Crystallized Zeolite Membrane,'' U.S. Patent No. 5,948,980 (1998).

Lai, W. F., H. W. Deckman, J. A. McHenry, and J. P. Verduijn, ''Supported Zeolite Membranes with Controlled Crystal Width and Preferred Orientation Grown on a Growth Enhancing Layer,'' U.S. Patent No. 5,871,650 (1999).

Li, J. Q., J. X. Dong, and G. H. Liu, ''Preparation and Properties of Zeolite Coating on Metal Surface,'' *React. Kinet. Catal. Lett*., **47**, 287 (1992).

Li, J. Q., J. X. Dong, and G. H. Liu, ''Preparation and Properties of a New Kind of Acid Catalyst of Zeolite Coating on Metal-Surface,'' *Stud. Surf. Sci. Catal*., **90**, 327 (1994).

Lovallo, M. C., A. Gouzinis, and M. Tsapatsis, ''Synthesis and Characterization of Oriented MFI Membranes Prepared by Secondary Growth,'' *AIChE J*., **44**, 1903 (1998).

Lovallo, M. C., and M. Tsapatsis, ''Preferentially Oriented Submicron Silicalite Membranes,'' *AIChE J*., **42**, 3020 (1996).

Matsukata, M., N. Nishiyama, and K. Ueyama, ''Preparation of a Thin Zeolitic Membrane,'' *Stud. Surf. Sci. Catal*., **84**, 1183 (1994a).

Matsukata, M., N. Nishiyama, and K. Ueyama, ''Zeolitic Membrane Synthesized on a Porous Alumina Support,'' *J. Chem. Soc., Chem. Commun*., 339 (1994b).

Mimura, H., T. Tezuka, and K. Akiba, ''Preparation of Analcime Film from Hydrogels,'' *J. Nucl. Sci. Technol*., **33**, 892 (1996).

Mintova, S., B. J. Schoeman, V. Valtchev, J. Sterte, S. Y. Mo, and T. Bein, ''Growth of Silicalite Films on Pre-Assembled Layers of Nanoscale Seed Crystals on Piezoelectric Chemical Sensors,'' *Adv. Mater*., **9**, 585 (1997a).

Mintova, S., V. Valtchev, V. Engstrom, B. J. Schoeman, and J. Sterte, ''Growth of Silicalite-1 Films on Gold Substrates,'' *Microporous Mater*., **11**, 149 (1997b).

Myatt, G. J., P. M. Budd, C. Price, and S. W. Carr, ''Synthesis of a Zeolite NAA Membrane,'' *J. Mater. Chem*., **2**, 1103 (1992).

Nishiyama, N., K. Ueyama, and M. A. Matsukata, ''Defect-Free Mordenite Membrane Synthesized by Vapor-Phase Transport Method,'' *J. Chem. Soc., Chem. Comm*., **19**, 1967 (1995).

Nishiyama, N., K. Ueyama, and M. Matsukata, ''Synthesis of Defect-Free Zeolite-Alumina Composite Membranes by a Vapor-Phase Transport Method,'' *Microporous Mater*., **7**, 299 (1996).

Nomura, M., T. Yamaguchi, and S. Nakao, ''Silicalite Membranes Modified by Counterdiffusion CVD Technique,'' *Ind. Eng. Chem. Res*., **36**, 4217 (1997).

Oh, H. S., M. H. Kim, and H. K. Rhee, ''Synthesis of ZSM-5 Zeolite Membrane on the Inner Surface of a Ceramic Tube,'' *Stud. Surf. Sci. Catal*., **105**, 2217 (1997).

Petersen, J., and K. V. Peinemann, ''Preparation and Gas Permeation Properties of Ceramic-Silicalite Membranes,'' *J. Mater. Sci. Lett*., **15**, 1777 (1996).

Piera, E., A. Giroirfendler, J. A. Dalmon, H. Moueddeb, J. Coronas, M. Menendez, and J. Santamaria, ''Separation of Alcohols and Alcohols/O-2 Mixtures Using Zeolite MFI Membranes,'' *J. Membr. Sci*., **142**, 97 (1998).

Raman, N. K., and C. J. Brinker, ''Organic Templated Approach to Molecular Sieving Silica Membrane,'' *J. Membr. Sci*., **142**, 97 (1995).

Ravishankar, R., C. E. A. Kirschock, P. Knops-Gerrits, E. J. P. Feijen, P. J. Grobet, P. Vanoppen, F. C. DeSchryver, G. Miehe, H. Fuss, B. J. Schoeman, P. A. Jacobs, and J. A. Martens, ''Characterization of Nanosized Material Extracted from Clear Suspensions for MFI Zeolite Synthesis,'' *J. Phys. Chem. B*, **103**, 4960 (1999).

Ruderman, W., J. R. Fehlner, and Z. Zhang, ''Synthesis of Inorganic Membranes on Supports,'' U.S. Patent No. 5,779,904 (1998).

Sano, T., Y. Kiyozumi, and M. Kawamura, ''Preparation and Characterization of ZSM 5 Zeolite Film,'' *Zeolites*, **11**, 842 (1991).

Sano, T., F. Mizukami, H. Takaya, T. Mouri, and M. Watanabe, ''Growth-Process of ZSM-5 Zeolite Film,'' *Bull. Chem. Soc. Jpn.*, **65**, 146 (1992a).

Sano, T., Y. Kiyozumi, F. Mizukami, H. Takaya, T. Mouri, and M. Watanabe, ''Steaming of ZSM-5 Zeolite Film,'' *Zeolites*, **12**, 131 (1992b).

Scandella, L., G. Binder, J. Gobrecht, and J. C. Jansen, ''Alignment of Single-Crystal Zeolites by Means of Microstructured Surfaces,'' *Adv. Mater.*, **8**, 137 (1996).

Schoeman, B. J., A. Erdemsenatalar, J. Hedlund, and J. Sterte, ''The Growth of Submicron Films of TPA-Silicalite-1 on Single-Crystal Silicon-Wafers from Low-Temperature Clear Solutions,'' *Zeolites*, **19**, 21 (1997).

Sterte, J., S. Mintova, G. Zhang, and B. J. Schoeman, ''Thin Molecular-Sieve Films on Noble-Metal Substrates,'' *Zeolites*, **18**, 387 (1997).

Tricoli, V., J. Sefcik, and A. V. McCormick, ''Synthesis of Oriented Zeolite Membranes at the Interface Between Two Fluid Phases,'' *Langmuir*, **13**, 4193 (1997).

Tsay, S. C., and A. S. T. Chiang, ''The Synthesis of Colloidal Zeolite TPA-Silicalite-1,'' *Microporous Mesoporous Mater.*, **26**, 89 (1998).

Uzio, D., J. Peureux, A. Giroirfendler, J. A. Dalmon, and J. D. F. Ramsay, ''Formation and Pore Structure of Zeolite Membranes,'' *Stud. Surf. Sci. Catal.*, **87**, 411 (1994).

Yan, Y. H., M. Tsapatsis, G. R. Gavalas, and M. E. Davis, ''Zeolite ZSM-5 Membranes Grown on Porous Alpha-Al_2O_3,'' *J. Chem. Soc., Chem. Commun.*, 227 (1995a).

Yan, Y. S., M. E. Davis, and G. R. Gavalas, ''Preparation of Zeolite ZSM-5 Membranes by In-Situ Crystallization on Porous Alpha-Al_2O_3,'' *Ind. Eng. Chem. Res.*, **34**, 1652 (1995b).

Zheng, C. S., J. L. Yin, S. H. Xiang, and H. X. Li, ''A Novel Preparative Route to a Silicalite Membrane,'' *Chem. Commun.*, 1285 (1996).

Manuscript received July 6, 1999, and revision received Oct. 8, 1999.